EARTH SURFACE PROCESSES AND LANDFORMS, VOL. 21, 103–123 (1996)

MID-CHANNEL BAR GROWTH AND ITS RELATIONSHIP TO LOCAL FLOW STRENGTH AND DIRECTION

PHILIP J. ASHWORTH

School of Geography, Leeds University, Leeds, West Yorkshire, LS2 9JT, U.K.

Received 30 June 1993
Accepted 2 March 1995

ABSTRACT

Anabranches of braided rivers typically migrate and avulse across the floodplain to produce new channel junctions, scour and subsequent mid-channel bar growth immediately downstream. Few quantitative studies have been made of this bar development process and the link to change in channel geometry and local flow strength and direction. This paper provides data on the spatial and temporal pattern of surface velocity as mid-channel bar growth is initiated downstream of a fixed junction scour in a generic scale flume model.

The sequence of channel changes is: (i) development of a confluence scour with flow convergence and maximum velocity in the channel centre; (ii) exceedance of the local transport capacity and initial stalling of coarse sediment in the channel thalweg downstream of the scour; (iii) bar growth through entrapment of all sizes of bedload; (iv) change from velocity maximum to minimum and flow convergence to divergence when the bar height is approximately 55 per cent of the thalweg depth; (v) broadening of the bartop platform, a drop in local competence and bankward migration of the two distributaries whose cross-section and velocity remains approximately constant.

These flume data and interpretations are compared to descriptions in the literature of the braiding process with particular reference to the flume work of Leopold and Wolman (1957) and Ashmore (1991, 1993). A new model for mid-channel bar growth is presented which helps explain the long-term development of the confluence–diffluence unit.

KEY WORDS braided rivers; bar growth; confluence dynamics; velocity distribution; flume modelling

INTRODUCTION

Gravelly braided rivers are characterized by high stream power, unconsolidated banks, non-uniform flow and bed topography, and rapid rates of erosion and deposition. Repeated dissection and reworking of the bed sediment leads to the preservation of a broad spectrum of bar forms (Smith, 1978; Church and Jones, 1982a), the two most common being the 'unit' or rhomboidal bar (Smith, 1974) and the 'compound' or mosaic bar (Bluck, 1979). Although it is difficult to define a unique relationship between the flow hydraulics and sediment supply responsible for the creation of each bar type (Church and Jones, 1982b; Jaeggi and Smart, 1982), undoubtedly one of the most favourable locations for bar initiation is immediately downstream of a channel confluence. Such sites are ubiquitous in braided rivers (Ashmore, 1993) and can be envisaged as a series of interconnected channels of 'X' and 'Y' planform that vary in length, asymmetry and sinuosity (Mosley, 1976; Carson and Griffiths, 1987; Ferguson and Ashworth, 1992). These confluence–diffluence morphologies are related to each other (the 'Y' shape is often a forerunner of the 'X') and form the chute–bar unit first described by Southard *et al.* (1984) and Davoren and Mosley (1986).

Many field and laboratory studies have described the temporal evolution of bars in these zones of alternating flow constriction and expansion (e.g. Leopold and Wolman, 1957; Krigström, 1962; Smith, 1974; Hein and Walker, 1977; Cheetham, 1979; Ashmore, 1982; Rundle, 1985; Davoren and Mosley, 1986; Fujita, 1989; Ashworth *et al.*, 1992a; Ferguson *et al.*, 1992; Goff and Ashmore, 1994). However, since channel change and depositional processes operate so rapidly in braided rivers, most of these studies have been

CCC 0197–9337/96/020103–21

either qualitative or confined to 'before and after' observations. An alternative approach has been to view the initiation of braiding as a stability problem with both linear (e.g. Engelund and Skovgaard, 1973; Parker, 1976; Fredsøe, 1978) and non-linear (e.g. Colombini *et al.*, 1987; Tubino, 1991) analyses of flow structure and sediment transport leading to definition of the critical criteria for braid–bar development. Unfortunately, the majority of current stability analyses only deal with bar growth in a single channel, which may not be representative of channel junction sites where two separate flows mix and a deep scour hole influences the three-dimensional flow structure and pattern of sediment dispersal. Therefore, despite these advances, little is known about the dynamics of the confluence–diffluence unit and in particular the influence of mid-channel bar growth on the local flow strength and direction (Ashmore, 1991, p. 338).

A number of advances have been made in quantifying the flow structure over point and alternate bars (e.g. Dietrich and Smith, 1983; Dietrich and Whiting, 1989; Nelson and Smith, 1989; Whiting and Dietrich, 1991), which are often seen as the precursors to braiding (Welford, 1994) and equivalent to one half of the back-to-back meander planform that resembles a distributary and mid-channel bar unit (Ashmore, 1982; Ashworth *et al.*, 1992b; Bridge, 1993). However, these models do not include the dynamics of mixing flows and may be inappropriate for the less sinuous distributary channels that are characteristic of braided rivers. Furthermore, the emphasis on the topographic forcing of flow by the bar morphology is more important in shallow flows, such as during the period of bar emergence, rather than the early stages of bar formation and rapid aggradation.

Clearly, more quantitative information is required on the interrelationship between flow, sediment transport and bar growth in a confluence–diffluence unit (Bristow and Best, 1993; Lane *et al.*, 1994). These relationships are complex, with substantial positive and negative feedback (Ferguson and Ashworth, 1992; Hassan and Church, 1992). It is therefore appropriate to set the experimental programme described here in context by presenting a working model of braid–bar evolution that combines existing ideas in the literature with new interpretations from the flume and field.

A MODEL OF MID-CHANNEL BAR GROWTH

Figures 1a–d show a model of mid-channel bar development downstream of a newly formed channel confluence. In an unconfined braidplain environment, channel avulsion is common and new channel junctions are frequently created (Figure 1a). In the case of a newly formed, symmetrical, 'Y' shaped confluence, with tributaries of equal water and sediment discharge, bar growth may be expected to start immediately downstream of the confluence scour zone (Figure 1b). The distance between the scour hole and initial bar growth is primarily a function of total discharge, tributary discharge ratio, sediment supply, junction angle and combined tributary channel widths (Mosley, 1976; Yalin, 1992) but other local factors may also be important (*cf.* Best, 1986).

If the incoming tributaries terminate at steep avalanche faces at the scour hole, significant flow separation will ensue (Mosley, 1976; Best, 1988; Best and Roy, 1991) which may then transform into a pair of back-to-back helical flow cells (Mosley, 1976; Ashmore, 1982; Ashmore *et al.*, 1992). Although the overall flow pattern is one of flow convergence towards the centre of the channel (Figure 1b; Yalin, 1992), the presence of helical cells can cause divergent secondary flows up to 35 per cent of the primary velocity near the bed (Ashmore *et al.*, 1992). Such secondary flows may be important in the confluence scour, but probably either break down in the higher width:depth ratios typical of barhead sites (Dietrich, 1987) or are transformed into a simple diverging flow throughout the water column as the flow shallows downstream (McLelland *et al.*, in press).

Selective deposition of the coarser fractions of the bedload in the channel centre signals the beginning of bar growth (Figure 1b) and modification of the local flow structure. The cause of this 'local sorting' (Leopold and Wolman, 1957, p.47) and subsequent deposition of the coarse fractions in the centre of the channel (where the velocity is at its highest) is still a topic of debate. Undoubtedly, the inwardly moving tributary flows will help transport particles into the thalweg and the convergence of bedload transport pathways around the scour hole (*cf.* Best, 1988) could lead to local exceedance of the transport capacity. Ashmore (1991) suggests that initial channel bar deposition is by the stalling of 'bedload sheets', with the coarse bar nucleus representing the downstream margin of the sheet as the larger particles outrun the finer ones.

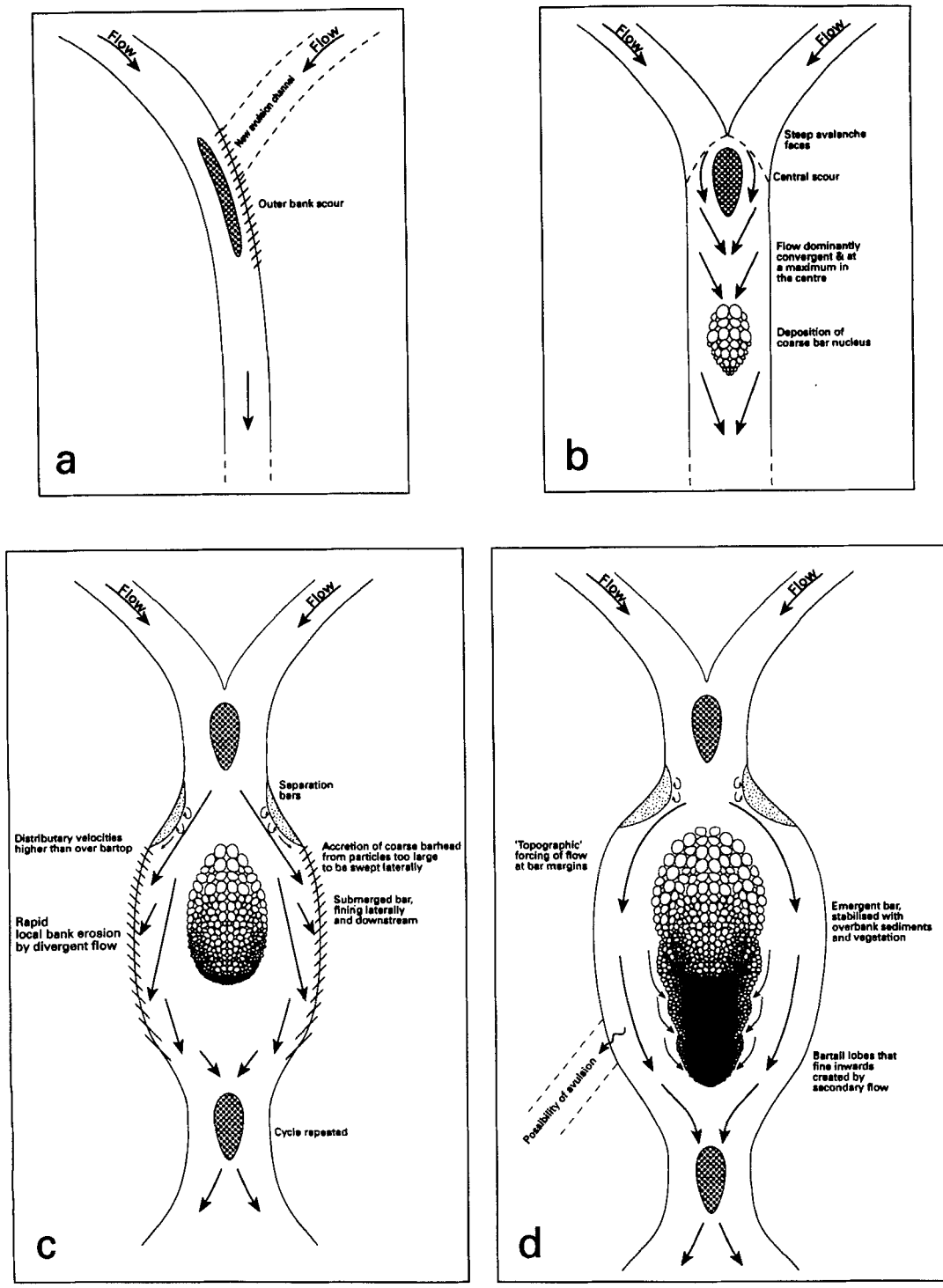

Figure 1. (a)–(d) Model of mid-channel bar growth downstream of a junction scour. The text contains a detailed description of each stage of bar development. Arrows refer to surface flow direction. The model is based on the work of Leopold and Wolman (1957), Mosley (1976), Ashmore (1982, 1991), Ashworth *et al.* (1992b) and observations from the field and flume

The initial stalling is brought about by a 'slight change in competence near the centre of the channel' (Ashmore, 1991, p. 334) which is plausible if the flow is shallow and close to critical. Recent work by McLelland *et al.* (in press) has shown that a core of high flow turbulence intensity or kinetic energy density exists in the centre of the channel immediately downstream of a confluence, but that this progressively lifts away from the bed and dissipates within a few channel widths downstream. This spatial redistribution of kinetic energy leads to a downstream reduction in the vertical energy gradient and therefore provides a zone for sediment accumulation and subsequent bar growth. More work is required on the precise combination of hydraulic and sediment transport factors that are responsible for initial mid-channel bar deposition. However, once started, the bar continues to grow by entrapment of all sizes of bedload, both on its margins and in the sheltered low velocity zone behind the coarse barhead (Figure 1b).

Eventually, the bar is large enough to deflect flow against the adjacent banks (Figure 1c), causing bank erosion, a decrease in average water depth, and hence a drop in reach-average shear stress. This change from flow convergence to divergence shifts the core of maximum velocity from the centre of the channel (and over the bartop) to the distributaries. This is also the stage at which the two distributaries around the mid-channel bar start to take over from the bartop as the principal corridors for bedload transport (Ashworth *et al.*, 1992b). The development of a new confluence–bar unit has an immediate impact on the downstream channel geometry (Figure 1c), with a series of constriction (scour) and expansion (bar) zones alternating down the channel as the flow repeatedly converges and diverges.

The decrease in competence caused by channel widening (Figure 1c) promotes further bar aggradation which in turn forces stronger flow divergence until the bar emerges and stabilizes (Figure 1d) or is dissected and starts the process over again, with an adjacent incipient bar forcing new flow divergence. The emergent mid-channel bar may stabilize through overbank sedimentation and vegetation (Leopold and Wolman, 1957) and/or undergo further modification (Figure 1d) through the successive addition of bartail scrolls by incoming secondary flows (Ashworth *et al.*, 1992b) or asymmetric growth as one of the distributaries is captured by a new avulsion at a bank weakness or floodplain topographic low (Ashmore, 1993; Leddy *et al.*, 1993).

This model of mid-channel bar growth draws heavily on the qualitative observations of laboratory flume work (in particular Leopold and Wolman (1957), Mosley (1976), Ashmore (1982, 1991) and Ashworth *et al.* (1992b)) and ignores many of the local hydraulic factors that may influence confluence–bar development. The symmetrical 'Y' confluence planform is one of the basic building blocks of braided rivers, but often develops asymmetrically over time as one of the tributaries or distributaries becomes more dominant. Bed scour, channel curvature (and hence bank erosion), armouring, and the capture of discharge from adjacent tributaries can lead to the preferential development of an individual anabranch (Hoey and Sutherland, 1991; Ashmore, 1993). Furthermore, the model depicted in Figures 1a–d is essentially a 'static' model (Ashmore, 1982) where migration of the mid-channel bar is not a prerequisite for continuation of braiding. Other models for braiding exist (see review by Ashmore, 1991) but it is deposition and accumulation as a mid-channel bar that is the most common mechanism in zones of flow constriction and expansion typical of intersecting braided channel networks (*cf*. Carson and Griffiths, 1987).

This simple working model of braid–bar development highlights the need to quantify the spatial and temporal pattern of velocity and flow direction as a mid-channel bar and confluence–diffluence unit evolves. The model raises several fundamental questions.

1. Does a bar start to grow in the zone of highest velocity downstream of a channel junction and is this zone in the centre of the channel?
2. How does channel cross-section geometry respond to bar growth and what is the feedback between mid-channel shallowing, distributary development and bank erosion?
3. Is there a change in the velocity magnitude over the bartop as compared to the distributaries whilst the bar aggrades? If so, is there a critical bar height which determines whether flow velocity is at a maximum or minimum over the bartop in comparison to the distributaries?
4. Does the spatial pattern of surface flow convergence/divergence change as a bar aggrades and how does this link to the changes in velocity magnitude?

This paper reports on a series of flume-scale experiments where bar growth is initiated downstream from a symmetrical channel confluence. Measurements of the spatial distribution of surface velocity are combined with surveys of bar aggradation to address the four questions above and test the validity of the general model of mid-channel bar development illustrated in Figures 1a–d.

MODELLING PROCEDURE

The principal advantages of physical scale modelling are comprehensively reviewed by Yalin (1971), Mosley and Zimpfer (1978), Ashmore (1982) and Ashworth *et al.* (1994). Although, theoretically, it is possible to produce a strict Froude-scale model of a field prototype whereby the dynamic, kinematic and geometric variables of the system are scaled exactly, the majority of fluvial scale models opt for a degree of flexibility and generality (e.g. Ashmore, 1982; Hoey and Sutherland, 1991; Warburton and Davies, 1994). These more popular 'generic' models (Ashmore, 1991) aim to preserve similarity in process with the prototype whilst not constricting the model to one specific case study. Generic models should still be verified against a field prototype, with particular care taken to ensure that the model has the appropriate range of flow roughness and turbulence, but they do not require an exact match between model and prototype hydraulic and geometric variables.

Generic modelling principles are followed in the experiments reported here. The field prototype is the proglacial, braided White River in Mount Rainier National Park (Washington State, U.S.). A detailed description of the catchment and river characteristics is given in Ferguson *et al.* (1989). Measurements of the flow hydraulics and channel geometry for a 40 m long study reach are summarized in Table I. Mean velocity and bed shear stress were measured at-a-point using a vertical array of simultaneously recording propeller current meters (see Ashworth and Ferguson, 1989). These data represent an amalgamation of velocity profiles collected at different positions in the reach during three days of high snowmelt floods, when flows were close to bankfull. Fieldwork in the White River preceded the flume experiments and allowed the geometric and

Table I. Comparison of modelling criteria between the flume and the White River prototype. The model employs a length scale of 1:30. Flow in the model is fully rough and turbulent but largely supercritical (see text for further information)

			Model		White River prototype	
Symbol	Variable	Units	Mean	Range	Mean	Range
u^*	Mean velocity	$m\,s^{-1}$	0·48	0·30–0·65	1·38	0·63–2·09
Y	Water depth	m	0·015	0·0065–0·023	0·48	0·22–0·85
W	Maximum channel width	m	0·64	n.r.	24·4	n.r.
S	Slope	–	0·016	n.r.	0.016	n.r.
Q	Water discharge	$m^3\,s^{-1}$	0·00297	0·00184–0·00452	6·91†	n.r.
Q_s‡	Sediment discharge	$g\,m^{-1}\,s^{-1}$	4·37	0·0981–22·1	98·1	0·10–812
ρ_s	Sediment density	$kg\,m^{-3}$	2600	n.r.	2590	n.r.
Y/D_{90}	Relative roughness	–	3·46	1·41–5·00	2·69	1·33–5·21
Fr§	Froude number	–	1·27	0·64–1·89	0·64	0·39–1·03
Re¶	Flow Reynolds number	–	8660	3580–14500	444 000	86 600–1 020 000
Re||	Grain Reynolds number	–	349	178–586	32 500	12 100–49 100

n.r. = no range

• The hydraulic data were obtained from 36 velocity profiles taken in the flume and 62 in the field. The White River data were obtained for a reach 2 km downstream of that described in Ferguson *et al.* (1989) and are documented in Ashworth (1988)

† Maximum discharge only (when most measurements were taken)

‡ Transport rate calculated for fractions coarser than 7·5 mm (scaled-up model grain size) and 8 mm (prototype). Data obtained from 106 Helley-Smith samples in the flume and 52 in field. More details on the flume data are available in Ashworth *et al.* (1992b)

§ $Fr = u/(gY)^{0.5}$

¶ $Re = uY/\nu$, where ν is the fluid kinematic viscosity (flume = $8{\cdot}7 \times 10^{-7}\,m^2\,s^{-1}$, field = $1{\cdot}6 \times 10^{-6}\,m^2\,s^{-1}$)

|| $Re* = (\tau/\rho)^{0.5} D_{90}/\nu$, where τ is the at-a-point bed shear stress calculated from pitot tube velocity profiles and the 'Law of the Wall'

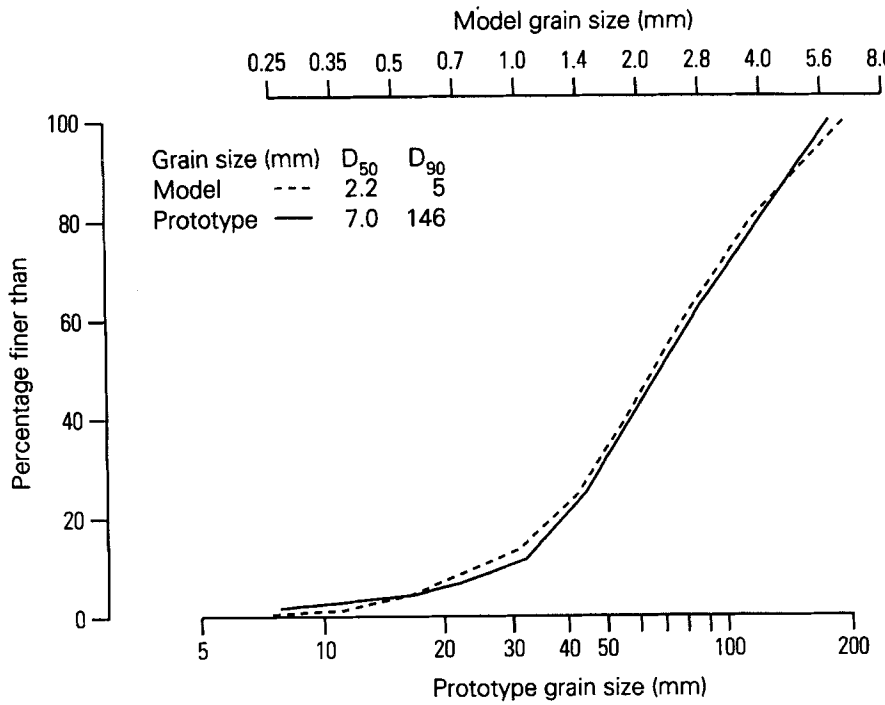

Figure 2. Flume model and field prototype sediment grain size. The flume model uses a length scale of 1:30 and is based on the proglacial White River

hydraulic properties of the model to be set within the range measured in the prototype. In order to maximize the size of the model in the 0·9 m wide flume (whilst maintaining the flow and grain Reynolds numbers in the appropriate range), a length scale of 1:30 was selected. This scaling ratio was used to produce a model grain size distribution equivalent to that obtained from a 64 kg bulk grain size sample of the White River bed surface. Figure 2 shows that an excellent match was obtained between model and prototype. Truncation of the model grain size distribution at 0·25 and 5·7 mm was necessary due to commercial constraints on the sand supplied, but still enabled 96 per cent of the White River bed grain size to be represented in the model.

Table I also shows the range of model hydraulic and geometric variables measured during the flume runs. Estimates of model mean velocity, Froude number and flow and grain Reynolds number were obtained from 36 velocity profiles taken at 50 mm intervals along two cross-sections at the barhead using a 2 mm diameter pitot tube. Velocity profiles were taken up to the water surface and are generally logarithmic (mean $r^2 = 97{\cdot}7$, range 92·2–99·8). Hence, they are used as a reliable estimate of bed shear stress and mean velocity using the log law and integration of the velocity profile.

Comparison of the key hydraulic and geometric variables shown in Table I indicates that there is a close agreement between model and prototype. In all cases the flow was fully turbulent (flow Reynolds number >2000) and rough, with viscous forces being minimal (grain Reynolds number >70). Froude numbers in the model indicate flow that is transitional between sub- and supercritical but with a mean greater than unity. Although not matched by the White River field data (because most velocity profiles were taken in the channel thalwegs), these model Froude numbers are not unrealistic for braided rivers, which commonly have trains of standing waves on the water surface (Williams and Rust, 1969; Boothroyd and Ashley, 1975; Church and Gilbert, 1975), indicating local supercritical flow. Furthermore, most other braided flume studies report Froude numbers greater than unity (e.g. Ashmore, (1991), mean $Fr = 1{\cdot}13$, range 0·91–1·30; Hoey and Sutherland (1991), mean $Fr = 0{\cdot}90$, range 0·58–1·54).

The flume model is a generic analogue of a braided river reach. With a length scale of 1:30, the model water

depths are equivalent to a mean of 0·45 m in the field and a maximum channel width of 19·2 m. The similarity between the hydraulics, channel geometry (Table I) and bed grain size (Figure 2) between the model and prototype suggests that the experiments do closely resemble braided river field conditions.

FLUME SET-UP

Six runs (termed 1–6) were undertaken in a 0·9 × 11 m tilting flume. Water is stored in a 1 m^3 feeder tank which, when overtopped, enters the flume via a series of grills installed to generate turbulent flow. A fixed wooden structure was constructed to channelize the discharge into two feeder tributaries which are designed as half-width equivalents of the post-confluence channel. Figure 3 shows a plan view of the initial channel geometry. Metal guiding plates were installed along the outer banks of the two tributaries to fix the position and angle of the confluence (95°). All measurements are concentrated in the area where the first bar evolved (~ 50 cm downstream of the confluence, see Figure 3) but successive confluence–bar units were observed to develop along the entire flume length.

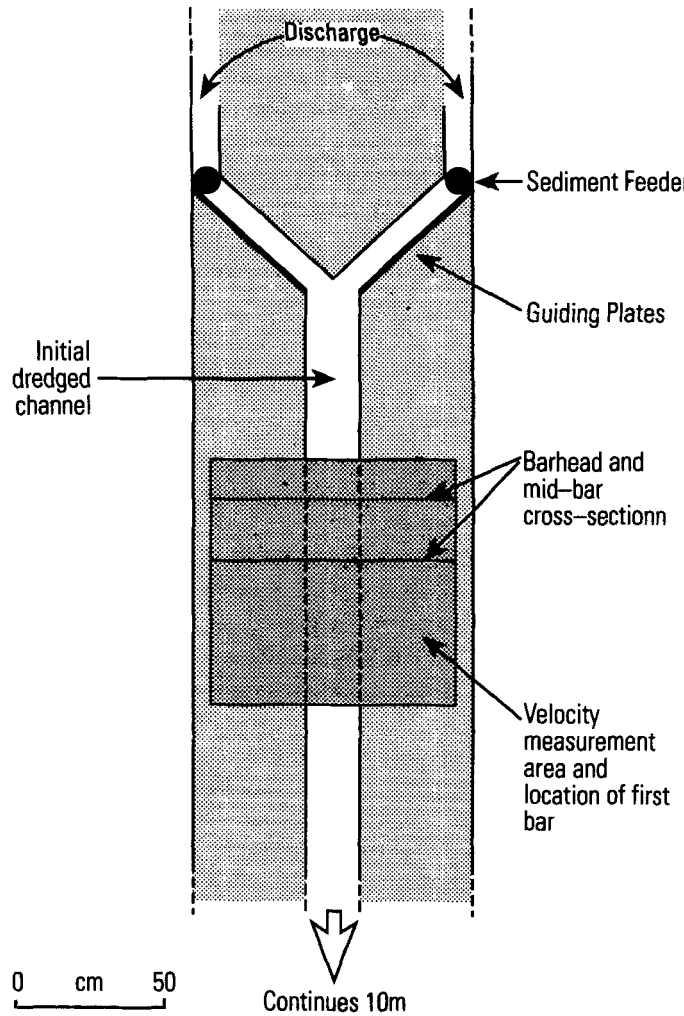

Figure 3. Plan diagram of the flume experimental set-up. Two half-width channels converge to produce a scour hole and mid-channel bar immediately downstream. Repeat cross-section surveys are combined with measurement of the surface velocity magnitude and direction to quantify the change in channel geometry and flow pattern at different stages of bar emergence

The scaled prototype sediment was thoroughly mixed and levelled to 100 mm depth along the flume. The same dry sediment was supplied to each feeder channel via two clear plastic tubes (Figure 3). Each tube had a serrated base and rested on the channel bed. Sediment supply rates were therefore dependent on an equilibrium between flow capacity and bedload supply, with the flow removing only the volume of sediment that it had the capacity to transport. Feed rates ranged from 1 to 8 g s^{-1}. Both water and sediment exited the flume into a box trap and were not recirculated. Draw-down effects were only present in the bottom 1 m of the flume.

DATA COLLECTION AND REDUCTION

The flume preparation and measurement procedure was identical for each flume run. A 250 mm wide, 35 mm deep, straight trapezoidal channel was dredged along the flume using a template fixed to a movable bridge. Flow was allowed to run for a few minutes to remove any loose sediment before measurements began. Preliminary experiments showed that a mid-channel bar would develop at approximately the same distance downstream from the confluence for successive runs. As described earlier, this is consistent with the findings of Mosley (1976) and Yalin (1992), who highlighted the importance of tributary discharge ratio, junction angle and total tributary width as some of the key factors controlling scour development and the position of downstream bar growth. Since these factors were fixed during the six experiments, the position of initial bar growth was identical in all runs. Water discharge was held constant in runs 3 and 4 but progressively raised in all other runs in order to increase the magnitude and rate of bar aggradation and assess the influence of a different channel-wide velocity on the spatial pattern of velocity and rate of bar growth (see later).

Two measurement cross-sections were defined at the predicted sites of barhead and mid-bar growth. These were 200 mm apart (Figure 3). Each section was surveyed using a point gauge fixed to a trolley mounted on rails. Heights of the bed and water surface were taken to ±0·1 mm at 30 mm intervals across-stream. A small viewing glass aided vision of the bed. Immediately following the survey of both cross-sections, a number of circular, fluorescent, polystyrene floats, 6 mm in diameter, were released simultaneously across the entire width of the channel upstream of the bar. Use of powerful lighting and an exposure time of 0·125 s on a 35 mm camera mounted directly above the channel provided photographs of the float transport paths as they moved through the measurement area. At least four sets of floats were released for each stage of bar growth. Transparencies of the photographs were projected onto a digitizing tablet, and the length, direction and midpoint coordinate of each float trace was recorded. Flow direction was defined relative to the centre of the channel (always parallel to the flume walls) and the float traces converted to velocity using the known camera exposure time and digitized float lengths.

The degree of emergence of the developing mid-channel bar is quantified using an index of bar growth illustrated in Figure 4. The original bed surface is defined as a parabolic cross-section of maximum depth equal to the initial dredged channel. The height of bar growth is then expressed as the ratio of the maximum bar height above this datum to the sum of the bar height and local water depth (in percentage terms). The bar growth index (BGI) is calculated for both measurement cross-sections and then averaged. The timing of cross-section measurement and float release was not the same for each experimental run but was selected to provide at least three stages of channel change and bar growth. Calculation of the BGI is straightforward if the channel is regularly shaped with a symmetrical bar, but becomes more problematic if the channel has two distributaries with unequal depths, or a compound bar with several undulating barhead lobes. This situation may be more common in the field but did not arise in any of the flume runs reported here.

In order to quantify the influence of mid-channel bar growth on the local flow strength and direction, it is necessary to differentiate between the zone of flow over the bartop and that in the two distributaries. It is often difficult to define exactly where such a boundary exists, since low relief mid-channel bars tend to grade into the adjacent distributary channels. The distributaries are defined here as 25 per cent of the cross-sectional width from both the left and right bank edges, and the bar zone as 12·5 per cent of the width either side of the channel centreline (Figure 4b). The cross-sectional width is the mean of the two measurement cross-sectional widths. This definition permits comparison of velocity datasets both within and between experimental runs, and ensures that the average surface velocity over the bartop is calculated using only

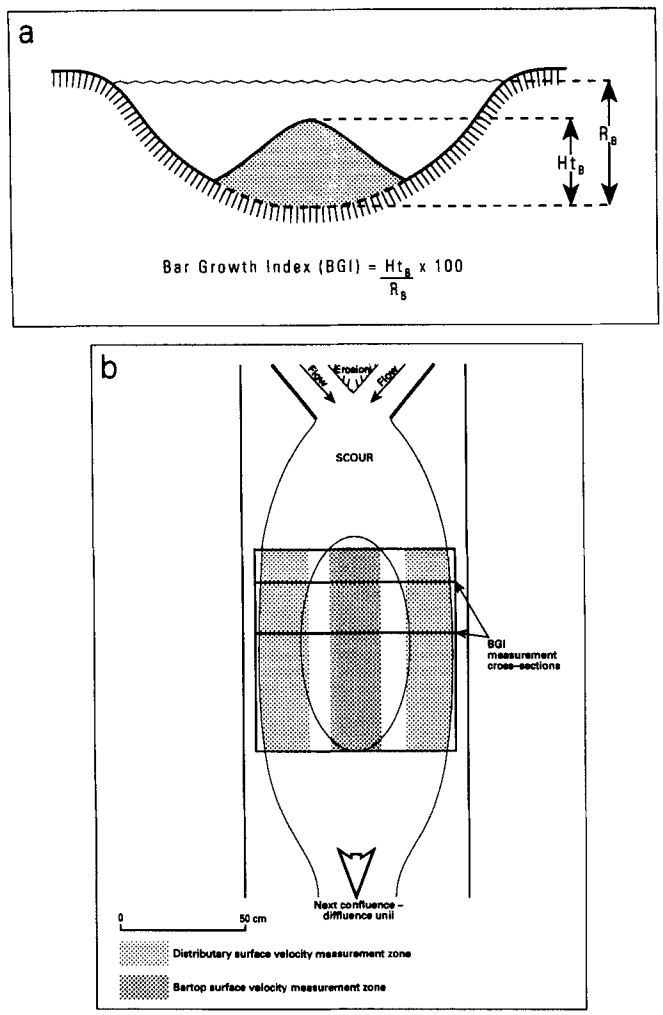

Figure 4. Definition of (a) the bar growth index (BGI), and (b) the areas of bartop and distributary for surface velocity measurements. The text contains an explanation of both definitions

the float vectors relating to the main bar nucleus. Since the mid-channel bar always developed symmetrically, with its margins approximately parallel to the flume walls at the cross-section sites, the use of a rectangular velocity measurement area clearly defines the zones of bar and distributary velocity (see Figure 4b). There was no systematic difference in the velocity magnitude in either of the competing distributaries, so the velocity vectors were combined and averaged. The velocity vector measurement area extended from immediately upstream of the barhead to the bartail (Figure 4b), although the majority of velocity traces were in the head to mid-bar region.

CHANGES IN CROSS-SECTION GEOMETRY DURING MID-CHANNEL BAR GROWTH

Table II contains a summary of experimental conditions for each of the six runs. Since the discharge was increased in runs 1, 4, 5 and 6, and the time between successive cross-section surveys is different, the magnitude of channel geometry change expressed in Table II must be viewed with caution. Nevertheless, two consistent trends can be observed: the process of bar growth is accompanied by both a progressive increase in

Table II. Experimental information for the six flume runs and summary statistics for wetted channel geometry and surface flow velocity measurements at different stages of mid-channel bar growth. Channel centre and distributary are defined as 25 per cent of the mean cross-sectional width at the bar centreline and from each bank edge respectively (see Figure 4b and text for more details)

Run number	Time elapsed since start (min)	Discharge ($l s^{-1}$)	Mean wetted channel			Mean surface velocity in centre ($cm s^{-1}$)	Standard error	N	Mean surface velocity in distributaries ($cm s^{-1}$)	Standard error	N	Velocity ratio (centre/ distributaries)	Bar growth index (BGI)
			Width (cm)	Depth (mm)	X-sec area (cm^2)								
1a	40	1·84	27·1	16·6	45·0				No measurements taken				
b	80	3·01	36·8	17·1	65·2	71·5	3·42	6	57·3	3·55	12	1·25	18·2
c	95	3·01	44·6	14·2	63·1	59·6	1·11	10	57·9	1·68	21	1·02	39·3
d	210	3·01	56·7	13·7	77·6	40·8	2·31	18	58·2	1·38	30	0·70	69·3
e	250	3·01	60·2	12·9	77·6	33·3	3·19	12	50·5	2·89	17	0·66	85·4
2a	20	2·42	29·5	20·7	61·2	65·0	1·11	16	56·4	4·00	11	1·15	0·0
b	60	2·42	32·8	18·5	60·6	65·6	1·43	23	56·8	2·37	7	1·15	27·9
c	105	2·42	46·9	15·4	72·4	44·4	1·78	45	56·1	2·48	25	0·79	56·5
d	135	2·42	51·6	13·5	69·5	17·1	2·24	21	35·6	2·99	59	0·48	73·7
3a	10	3·82	27·5	25·4	69·8	67·9	1·73	23	59·1	3·86	14	1·15	0·0
b	45	3·82	32·2	21·4	69·0	54·8	1·66	10	53·1	2·24	17	1·03	14·3
c	100	3·82	42·8	16·8	71·4	54·5	1·01	28	54·6	1·12	20	1·00	53·4
d	190	3·82	63·9	16·0	102	31·7	2·75	19	53·3	0·99	49	0·59	78·2
4a	15	2·16	31·1	18·5	57·4	65·8	2·34	10	56·0	2·00	17	1·18	15·0
b	50	2·16	33·8	16·9	57·2	58·9	0·89	17	55·9	1·35	26	1·05	14·7
c	145	2·76	44·3	15·8	69·9	53·0	1·14	42	50·0	1·37	35	1·06	39·9
5a	20	2·76	32·8	24·4	80·1	54·5	1·03	36	46·9	1·78	22	1·16	17·5
b	75	2·76	42·7	19·5	83·3	57·0	0·82	42	42·5	2·18	12	1·34	21·0
c	135	3·77	52·2	19·6	102	52·5	0·91	44	47·6	0·87	26	1·10	49·0
6a	25	2·42	32·2	19·4	62·5	58·0	0·95	14	52·2	2·38	14	1·11	0·0
b	65	2·76	42·4	18·8	79·6	59·9	0·96	35	54·5	1·11	17	1·09	27·2
c	150	4·52	60·5	19·3	117	63·3	0·76	44	62·4	0·96	18	1·01	51·6

All runs at slope = 0·016

Table III. Change in cross-sectional geometry as a mid-channel bar grows. The data are averaged for the two measurement cross-sections at the barhead and mid-bar region shown in Figure 4b. Only periods where the discharge is held constant are included (see Table II). The period of initial channel development up to the first set of cross-section measurements is excluded because the channel was reworking local loose sediment and weak bank material. The channel bed and water surface were surveyed using a point gauge (±0·1 mm) at 30 mm intervals across the measurement sections

Run period	Rate of wetted cross-section widening* ($mm\,h^{-1}$)	Rate of change in mean water depth† ($mm\,h^{-1}$)	Rate of change in wetted cross-sectional area‡ ($mm^2\,h^{-1}$)	Bar growth index range
1b–1c	+312	−11·6	−840	18–39
1c–1d	+63	−0·3	+756	39–69
1d–1e	+53	−1·2	0	69–85
2a–2b	+50	−3·5	−90	0–28
2b–2c	+188	−4·1	+1572	28–57
2c–2d	+94	−3·8	−580	57–74
3a–3b	+94	−7.8	−160	0–14
3b–3c	+116	−5·0	+262	14–53
3c–3d	+140	−0·5	+2040	53–78
4a–4b	+46	−2·8	−34	15–15

* Positive values = bank retreat
† Negative values = shallowing
‡ Positive values= enlargement

channel width and a decrease in mean water depth. Table III shows the rate of this cross-sectional change for consecutive measurement periods when the discharge was held constant. The change in wetted cross-sectional area for all runs is primarily a function of bank retreat and bar aggradation. However, Table III shows that there is a poor correlation between the rate of widening, shallowing and the degree of bar emergence (expressed by the range in BGI values), and also the direction of channel capacity change (increase or decrease) and the stage of bar and distributary development. The period of highest constant discharge (runs 3a–d) did produce the maximum amount of cross-sectional aggradation, and there is a tendency for wetted cross-sectional area reduction in the early stages of bar aggradation and then a change to overall enlargement once the bar occupies a major proportion of the local flow depth. However, the data in Tables II and III clearly show that the morphological response of a confluence–diffluence unit to bar creation and evolution is both non-uniform and highly variable. The rates of widening and shallowing for all runs are generally of the same order of magnitude, but they produce rates of cross-sectional change that switch from positive to negative and are spread over three orders of magnitude.

One of the few studies that provide comparable data on the mode of mid-channel bar evolution at a constant discharge is the flume work of Leopold and Wolman (1957). Unfortunately, only the cross-sections from two experiments are plotted by Leopold and Wolman (runs 6–8, fig. 34, p. 46 and run 17, fig. 37, p. 49). However, these runs and cross-sections are important because they are central to Leopold and Wolman's classic description of the braiding process which has subsequently become embedded in the fluvial literature. Table IV summarizes the digitized changes in cross-sectional geometry for two survey lines over the developing mid-channel barhead in these runs.

Runs 6–8 show bank erosion at the site of mid-channel bar growth but at rates much lower than those measured in the flume experiments described above (possibly because the average stream power is lower in the experiments of Leopold and Wolman). The mean water depth decreased as bar growth proceeded (again, at rates much lower than shown in Table III), but there was no consistent form of wetted cross-sectional change (it initially enlarged and then shrank as the bar emerged). The relationship between channel capacity and bar growth is even more complicated in run 17 (Table IV). Despite the growth of a mid-channel bar, which occupied up to 50 per cent of the channel width, negligible bank erosion occurred and was confined solely to the zone of barhead accretion. Instead, bar growth was accompanied by distributary

Table IV. Change in cross-section geometry as a mid-channel bar grows. Data are obtained from digitizing repeat cross-section surveys of a laboratory flume model published in Leopold and Wolman (1957). The experimental conditions for runs 6–8 are: constant discharge = 2·41 l s^{-1}, slope = zero, median grain size = 0·838 mm. Experimental conditions for run 17 are: constant discharge = 0·28 l s^{-1}, slope = 0·0103, median grain size = 0·749 mm. More details in Leopold and Wolman (1957, appendix C, p. 76). The cross-section for runs 6–8 is at Station 14 (barhead) and for run 17 at Station 6 (barhead). The mid-channel bar is emergent after 10 h in runs 6–8 so the final cross-section at 18 h is excluded. Likewise, the last cross-section measurement after 11·2 h in run 17 is omitted because the barhead had migrated downstream of the section. The timing of the cross-section measurement in run 17 stated by Leopold and Wolman (1957, fig. 37, p. 49) is difficult to interpret so the precise digital time given above each section is used to calculate the rates of cross-sectional change. The bar growth index is calculated in the same manner as the flume experiments reported in Table II (see Figure 4a)

Run period	Time period (h)	Rate of wetted cross-section widening* (mm h^{-1})	Rate of change in mean water depth† (mm h^{-1})	Rate of change in wetted cross-sectional area‡ (mm^2 h^{-1})	Bar growth index range
6–8	0–4	+27	−0·39	+99	0–85
6–8	4–10	+17	−0·76	−226	85–100
17	1·5–4·3	+3·5	−0·14	−19	0–87
17	4·3–7·2	+1·3	+0·11	+0·49	87–64

* Positive values = bank retreat
† Negative values = shallowing
‡ Positive values = enlargement

incision and intermittent bar degradation as the band of active sediment transport migrated across and down the channel. Table IV shows that survey station six at the barhead experienced very low rates of cross-sectional change and, similar to the experiments described in Tables II and III, alternated between periods of channel capacity reduction and enlargement.

The results in Tables II–IV highlight the complex relationship that exists between mid-channel bar growth and local morphological change. New bar aggradation (whether through vertical or lateral accretion) does not necessarily lead to a corresponding increase in channel width or distributary depth in order to accommodate the constant water discharge (i.e. the wetted cross-sectional area does not always stay constant). If there is such an imbalance, there must be an impact on the mean channel-wide velocity distribution (see below). The results show that bank erosion may be accelerated through deflection of the primary velocity by the gross bar morphology (see Figure 1c) but this may also be accompanied by distributary incision or overall cross-sectional aggradation.

CHANGES IN SURFACE VELOCITY DISTRIBUTION DURING MID-CHANNEL BAR GROWTH

As the discussion above has highlighted, mid-channel bar growth not only causes changes in the spatial and temporal pattern of bed and bank erosion but may also influence the channel-wide distribution of flow velocity. Table II summarizes the average surface velocity for the bartop and channel distributaries for different stages of bar growth in the six flume runs. In all cases, the standard error of the mean surface velocity is low (mean = 3·8 per cent, range 1·5–13 per cent). Runs of constant discharge show a general pattern of velocity decrease over the bartop with bar emergence (e.g. runs 3a–d, 67·9–31·7 cm s^{-1}) but largely unaltered mean distributary velocities (e.g. runs 3a–d, 59·1–53·3 cm s^{-1}). In light of the preceding discussion on channel geometry, these observations suggest that bar growth has little influence on the *distributary* cross-sectional form. In order for the distributary velocities to stay approximately constant during bar growth (Table II), their cross-sectional area must also remain constant (i.e. bank retreat must be matched by an equal area of lateral accretion of the bar margin). Thus, the decrease in bartop velocity is a product of both local shallowing as the bar emerges and a broadening of the bar platform. The non-uniform change in wetted cross-sectional area (Table III) is probably a product of the temporal and spatial lag in sediment supply, transport and

deposition on the bartop rather than variations in the cross-sectional form of the distributaries. Once the bar and distributaries are clearly defined, bar growth leads to the simple progressive bankward migration of the distributaries without modifying either their cross-sectional area or average velocity.

The ratio between mean surface velocity at the channel centre and distributaries for different stages of bar growth is plotted in Figure 5, with the division between bartop velocity maximum and minimum superimposed at a ratio of 1·0. Although the water discharge is different in each of the six flume runs and changed within four of the runs, Figure 5 shows that there is a consistent relation between the ratio of bartop to distributary velocity and the degree of bar emergence. In all runs, the ratio of bartop to distributary velocity is greater than unity (but below 1·4) until the BGI exceeds approximately 55 per cent (see Figure 5). As bar growth continues beyond this height, the velocity maximum in the centre of the channel changes to a velocity minimum and vice versa for the distributaries. Although Figure 5 suggests that this change in velocity distribution is transitional, more data are required to define the exact shape of the relationship, and it is more reasonable to assume that there is a band between BGI values of 40 and 60 per cent for the velocity switch rather than one single value. Once the BGI exceeds 55 per cent, the bartop velocity decreases rapidly as the flow becomes shallower and the bar platform develops (Table II). The minimum velocity ratio obtained is 0·48 for a BGI value of 74 per cent (run 2d). Since the mid-channel bar did not become emergent in any of the runs (maximum BGI = 84 per cent, run 1e), the velocity distribution in the final stages of bar emergence is unknown.

The increase in water discharge during four of the runs permits an investigation of the timing of the velocity change on the bartop as the absolute channel-wide velocity changes. Preliminary results from runs 4c, 5c

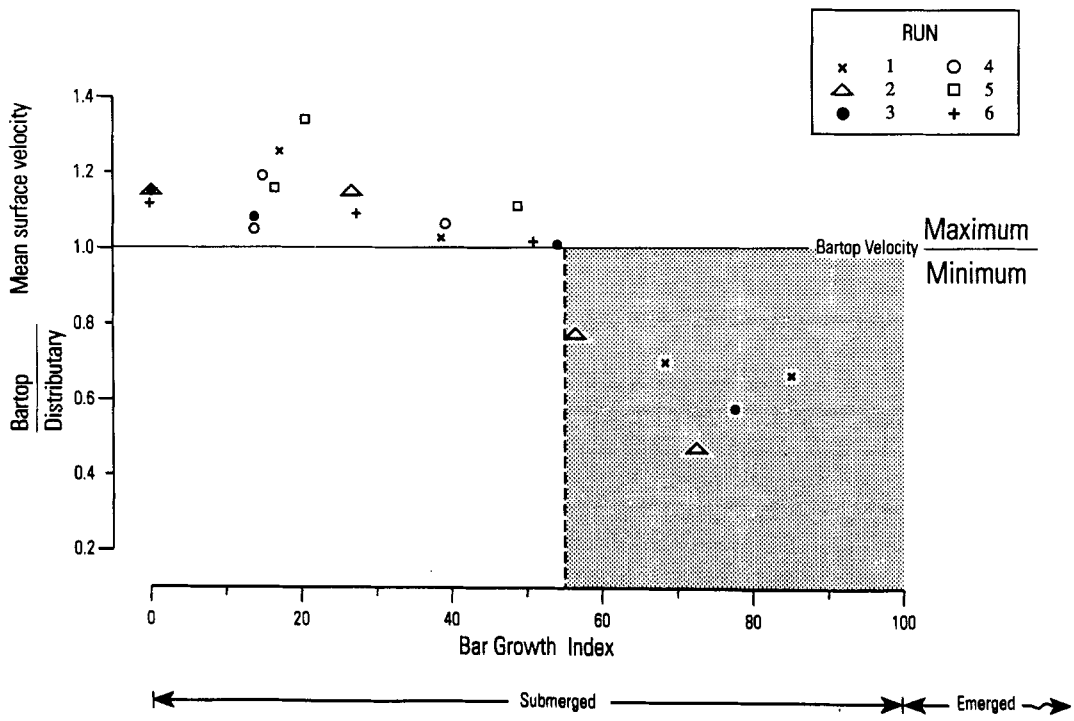

Figure 5. Change in the ratio of bartop to distributary velocity during mid-channel bar growth downstream of a junction scour. Standard errors of the mean velocities are given in Table II. The change from velocity maximum to minimum over the bartop occurs when the mid-channel bar reaches approximately 55 per cent of the local water depth (shown as shading). This change appears to be transitional rather than abrupt

and 6c suggest that an increase in discharge 'delays' the switch in velocity by reducing the local BGI (i.e. the increase in water depth initially outpaces the rate of bartop aggradation, see Table II). If there is also an increase in the absolute channel-wide velocity (e.g. run 6c), the ratio of centre to distributary velocity still remains within the expected range for the BGI value (i.e. the velocity ratio adjusts to the new BGI value). This suggests that the probability of maximum velocity switching is independent of the absolute velocity, and therefore that the flume results may be applied to rivers of different size, velocity and discharge, although more data are required.

The relationship between the degree of bar emergence and the ratio of bartop to distributary velocity is, by definition, strongly dependent on the flow stage. In natural environments, the discharge is not constant and the rate of mid-channel bar development is predominantly controlled by the local excess shear stress (which in turn is related to the position on the flood hydrograph) and the sediment supply. The flume runs discussed here change the BGI value and spatial distribution of velocity predominantly through bar aggradation. In the majority of field conditions, where sediment supply is restricted by catchment and tributary delivery processes, vegetation, bed armouring and cohesive bank material, the dominant control on the BGI value is more likely to be the flow stage and hydrograph shape. In this situation, a mid-channel bar may undergo two switches in velocity over its bartop: from a minimum to maximum as it becomes fully submerged (i.e. the bar morphology is 'drowned out' as the BGI drops below 55 per cent), and then maximum to minimum on the falling limb of the flood hydrograph. The timing and probability of the velocity switch is therefore a function of both sediment supply (i.e. bar aggradation) *and* water depth (i.e. flood hydrograph).

SPATIAL PATTERN OF SURFACE VELOCITY AND FLOW DIRECTION DURING MID-CHANNEL BAR GROWTH

The preceding section has highlighted the change in mean surface velocity for the two key zones of bar and distributary. However, it is unclear whether these two zones are isolated regions of high and low velocity, or areas of gradational velocity change. Furthermore, no quantitative detail has been given on the spatial pattern of flow direction and how this correlates with the change in the location of velocity maximum as bar growth proceeds. Velocity vectors for the four stages of bar growth measured during run 3 are shown in Figure 6. This run is selected as an example because the discharge was held constant throughout the measurement period and the mid-channel bar became almost emergent (BGI = 78 per cent for run 3d).

Figure 6 clearly shows the response of the flow strength and direction as bar growth proceeds and the channel widens. Reference to Table II indicates that run 3c represents the stage at which velocity switching is about to begin. By run 3d the mid-channel bar had aggraded to its maximum height for the local water depth, bedload transport had ceased and the bartop was an area of very low velocity (less than three times the mean distributary velocity).

Quantification of the channel-wide change in surface velocity is shown in Figure 7a. Each data point represents mean velocity over a 50 mm increment across the channel. In order to compare successive measurement periods of increasing bar and channel width, the cross-stream distance is made dimensionless through division by the mean cross-sectional width. During run 3a, a clear thalweg developed in the centre of the channel which possessed marginally higher velocities than nearer the banks (68 compared to 61 cm s^{-1}). Vectors at the bank edge highlight the role of bank friction on distributary velocity (see the channel extremes in Figure 6). Velocities are generally higher in the channel centre until run 3c, when two distinct peaks in the velocity distribution develop on the margins of the low relief bar. This is the first indication that the distributaries are beginning to take over as the cores of higher velocity. By run 3d the bar has aggraded to such an extent that the switch in velocity is marked. The channel centre now averages 24 cm s^{-1} and the two distributaries peak near 57 cm s^{-1}. The symmetrical appearance of the curve for run 3d in Figure 7a confirms that neither of the distributaries had the opportunity to become the dominant channel for conveying discharge. This may be the case for the initial aggradation and emergence of a mid-channel bar, but the longer-term evolution of a confluence–diffluence unit will usually result in one of the distributaries growing at the expense of the other (Cheetham, 1979; Hoey and Sutherland, 1991; Ashmore, 1993).

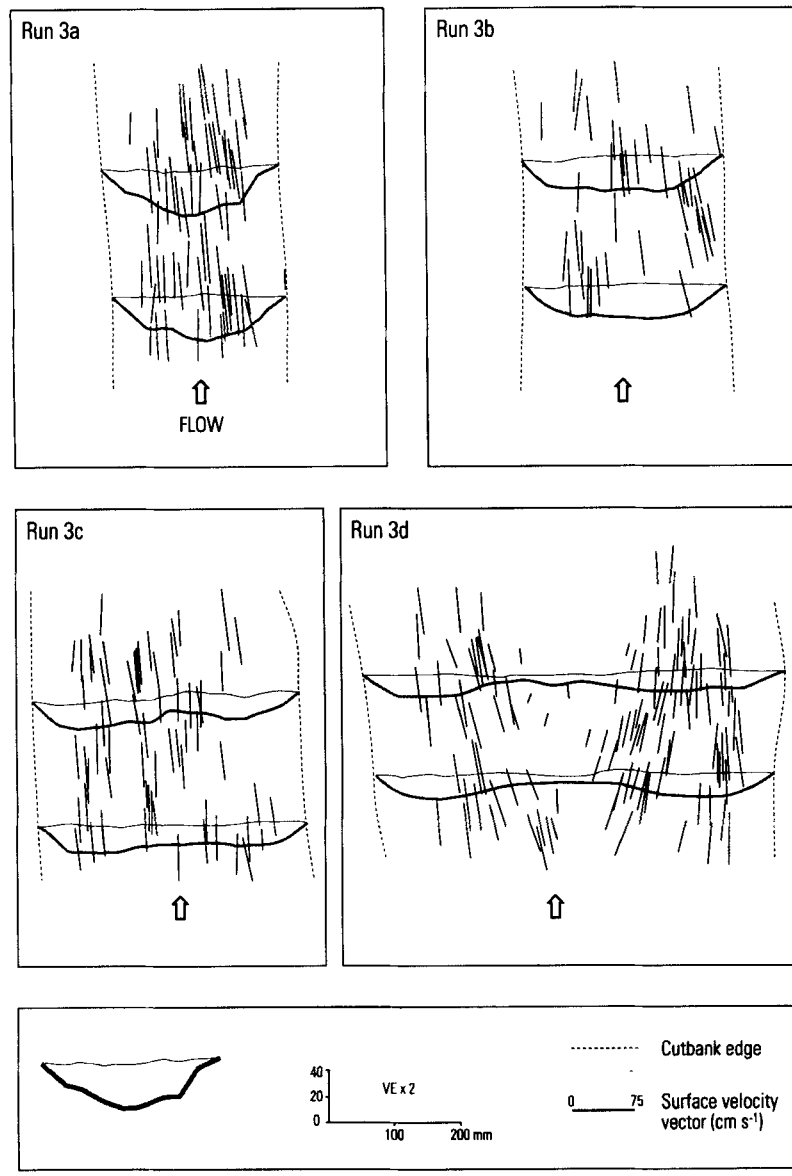

Figure 6. Temporal change in surface velocity magnitude and direction during mid-channel bar growth in run 3 (see Table II for more information). Run 3c is close to the point at which the bar is high enough to force a change from flow maximum to minimum and flow convergence to divergence over the bartop

Figure 7b quantifies the change in flow direction as bar growth proceeds. Flow is strongly convergent during run 3a, when the parabolic channel geometry steers the flow into the central thalweg. Although the angle of flow convergence is not entirely uniform across the channel width, run 3b and the right distributary of run 3c continue to show a surface flow direction towards the centre of the channel. Run 3c is the stage at which the influence of bar morphology on the spatial distribution of flow becomes apparent. Weak flow divergence is observed in the left distributary during run 3c, and by run 3d the bar deflects the majority of flow around its margins so that few floats travel over the bartop (see Figure 6). The degree of flow divergence is approximately symmetrical across the channel width, with maximum angles of 15° near the bar edges, decreasing

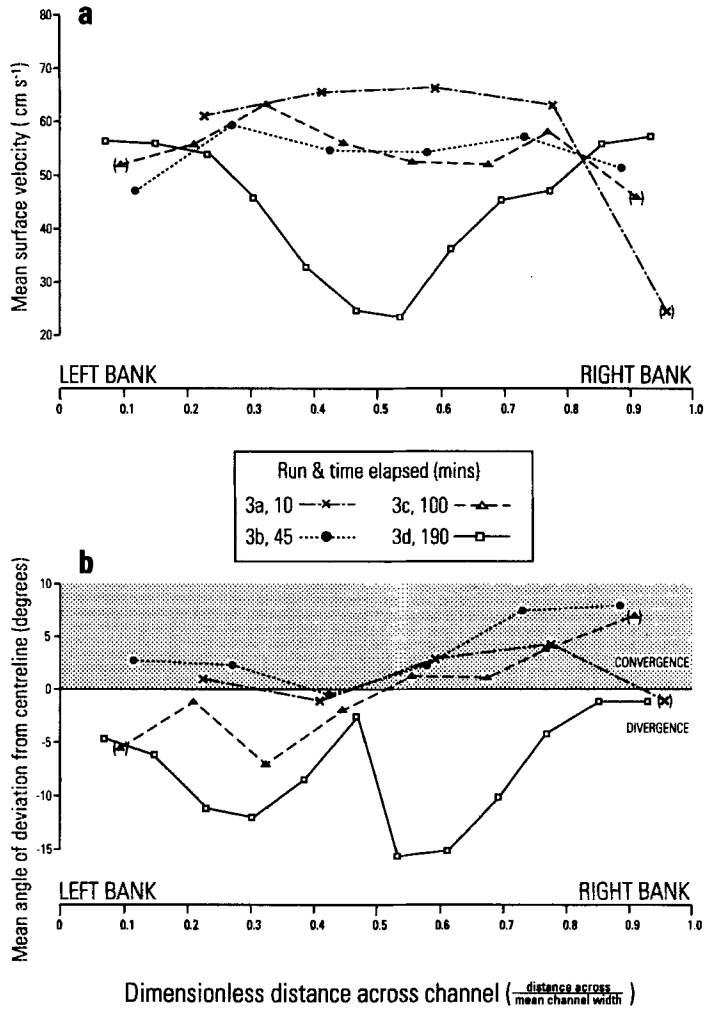

Figure 7. Channel wide distribution of (a) mean surface velocity, and (b) flow direction for run 3. Surface flow vectors shown in Figure 6 were digitized and averaged for 50 mm increments across the channel (i.e. in rectangular blocks across the measurement zone shown in Figure 3). Distance across the channel is taken as the middle of the 50 mm class made dimensionless through division by the average channel width.This enables comparison between runs of increasing channel and bar width. Data points with brackets only contain one vector and therefore may be unreliable. Note the simultaneous switch from velocity maximum to minimum and flow convergence to divergence at the channel centre by run 3d

bankwards as the deflected flow mixes with the faster and straighter distributary flow. The decrease in the rate of flow divergence from the bar to bank edge is gradual, but still maintains an outward component of between 2 and 5° at both bank margins. As discussed earlier, this divergent flow may fuel further bar growth through bank retreat and a subsequent decrease in average cross-sectional competence (Leopold and Wolman, 1957).

The maximum degree of flow divergence in run 3d (30° in total) is within the range suggested by Williams and Rust (1969) and Bridge and Gabel (1992) and mirrors the typical angles of barhead morphology found in natural braided rivers. There is a close match between the shape and cross-stream position of the curve for run 3d in Figure 7b and that in Figure 7a. This suggests that the change in velocity maximum to minimum in the centre of the channel as a bar grows is accompanied by a simultaneous change in flow convergence to divergence.

DISCUSSION AND SUMMARY

Anabranches of braided rivers frequently avulse across their floodplain to join neighbouring channels and produce a new channel confluence, junction scour and downstream mid-channel bar. Although the temporal evolution of this confluence–diffluence unit has been described qualitatively (see the work summarized in Figures 1a–d), up to now only the flume work of Leopold and Wolman (1957) has provided any quantitative information on mid-channel bar growth and its link to the braiding process. The generic flume experiments described here supplement these data and present the first geometric and flow measurements on the temporal evolution of a mid-channel bar in a straight channel downstream of a new channel junction. The flume runs differ from those of Leopold and Wolman (1957) and other stream table experiments (e.g. Ashmore, 1982, 1991) because two tributaries are forced to converge and create a confluence scour rather than allowing this to develop naturally. It is difficult to assess what influence this has on the evolution of the mid-channel bar and confluence–diffluence unit, but it probably increases the *rate* of development, as shown by comparing Tables III and IV. Certainly the process and format of mid-channel bar growth is very similar to that described by Ashmore (1982, 1991, 1993) and is probably similar to the situation of central bar formation in straight channels without any upstream flow convergence.

The flume experiments show that there is a complex relationship between mid-channel bar growth and flow strength, direction and morphological change. However, a number of common themes are apparent. Firstly, symmetrical tributaries with identical water and sediment discharge will develop a symmetrical mid-channel bar at a fixed distance downstream of the junction scour. The bar nucleus remains stationary during rapid vertical aggradation, but this may be attributable to the fixed tributary sidewalls which prevent scour hole migration. Bar growth did not involve any upstream barhead accretion (unlike the observations of other workers, e.g. Ashworth and Ferguson (1986), Carson and Griffiths (1987), Ashmore (1991), Lisle *et al.* (1991)), which supports the view of Leopold and Wolman (1957) that bar migration is not a prerequisite for bar growth and emergence.

A second issue is that there may be a specific degree of bar emergence when the velocity over the bartop changes from a maximum to minimum when compared to the distributaries. Although the flume data are limited, the results suggest that this change in velocity is transitional rather than abrupt (i.e. there is no critical threshold) and occurs between BGI values of 40 and 60 per cent, although 55 per cent may represent the average level (Figure 5). Further support for this comes from a recent field study reported in Hunt (1994). Measurements of surface velocity were taken in seven straight channels of a proglacial braided river, each containing a well developed mid-channel bar (not all downstream of channel junctions). The field programme was initiated to specifically test the relationship illustrated in Figure 5. The rationale for the flume experiments was applied in reverse by selecting a submerged 'mature' barform and taking velocity measurements over it and in the distributaries as the flow stage dropped. Figure 8 shows that the velocity ratio ranged from 0·17 to 1·38 and the BGI from 49 to 91 per cent. Although there is a fair degree of scatter (correlation coefficient, $r = -0{\cdot}75$), the data help support the flume observations shown in Figure 5. The relationship between bartop and distributary velocity is linear and the change from a velocity maximum to minimum over the bartop occurs at a BGI of 50·4 per cent (ordinary least-squares regression with intercept of 1·0).

Although no data are available for BGI< 49 per cent, the field results of Hunt (1994) support the hypothesis that the shift in velocity maximum from the bartop to distributaries occurs over a narrow range of BGI values and possibly between 50 and 55 per cent. Clearly more data are required, but the similarity between the data from the flume (with different discharges) and the field (for different bar and reach geometries) suggests that there may be a more widely applicable relationship between bar growth and the spatial pattern of flow velocity, which is independent of the magnitude of absolute velocity and scale of channel and bar size.

In contrast, the change in cross-sectional geometry as a mid-channel bar grows is highly variable. The flume results show that aggradation of the mid-channel bar certainly contributes to the divergence of flow, and shift in maximum velocity to the distributaries, and hence the acceleration of bank erosion. This relationship between mid-channel bar growth and bank erosion has been documented by Ashworth and Ferguson (1986), Thorne *et al.* (1993) and Goff and Ashmore (1994). However, mid-channel bar growth does not always lead to channel widening. This has been shown for one of the runs described by Leopold and

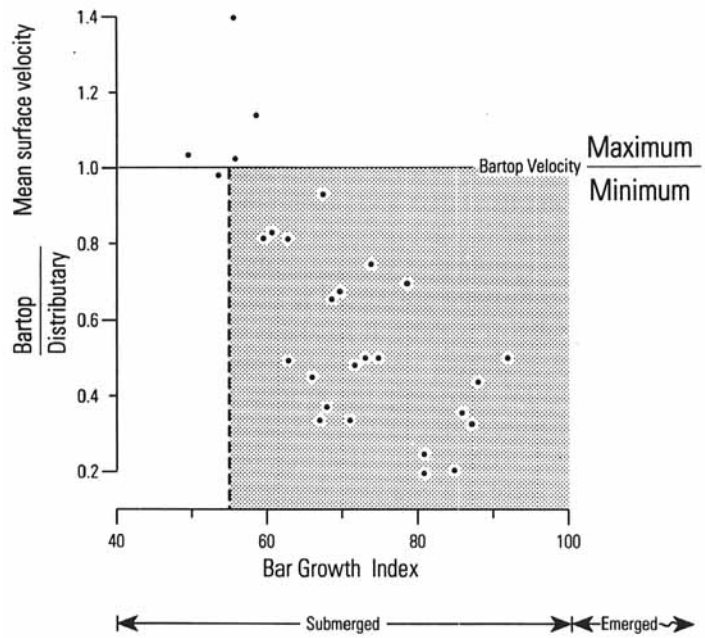

Figure 8. Identical plot to Figure 5 using the field data reported in Hunt (1994). Mean surface velocities were obtained from 15 s readings using an Ott current meter at 0·33 m intervals across the channel. The shaded area represents the stage at which the degree of bar emergence has caused a change in the bartop velocity from a maximum to minimum. Note that the division between bartop velocity maximum and minimum is approximately defined by a BGI value of 55 per cent, as shown by the flume experiments in Figure 5

Wolman (1957, Fig. 37, p. 49) but is also the case in an example of central bar formation illustrated by Ashmore (1991, fig. 5, p. 333). The flume data presented in Tables II and III suggest that the overall wetted cross-section fluctuates between periods of enlargement and reduction, but that the distributary cross-sectional area stays approximately constant. Broadening of the bar platform is accompanied by the progressive bankward migration of the distributaries, which continue to have the same channel capacity and average velocity. All flume runs experienced major bank retreat (usually a doubling of the initial channel width) but negligible distributary incision. Ultimately, the progressive shift from bank erosion to distributary incision is one of the ways in which a bar can become emergent at a constant discharge (Leopold and Wolman, 1957).

The data presented in Tables II–IV and Figures 5–8 support the two-dimensional model for mid-channel bar growth downstream of a confluence (Figures 1a–d) and provide quantitative information on the magnitude, timing and rate of bar growth, and related changes in flow strength and direction. Little attention has been given here to the relationship between the change in flow structure due to bar growth and the rate and size distribution of bedload transport. This topic is covered in Ashworth *et al.* (1992b) using bedload samples taken during the same flume runs reported here. However, it should be noted that as a mid-channel bar becomes more of an obstruction to the flow, it can steer or route different grain sizes along selective pathways over and around the barhead. The spatial pattern of bedload transport and grain size distribution is not only influenced by the flow strength and direction but also by the sediment supply (Ashworth *et al.* 1992a) and exact morphology of the barhead which topographically sorts the bedload (Parker and Andrews, 1985; Paola, 1989).

The model for mid-channel bar growth (Figures 1a–d) and flume results presented here only interpret the spatial and temporal pattern of *surface* velocity magnitude and direction. Although recent studies have shown that there may be significant secondary flows at confluence sites (e.g. Ashmore *et al.*, 1992; McLelland *et al.*, in press), which will cause marked deviations in the near-bed and surface flow strength and direction (Thompson, 1986), it is assumed that these effects are minor in the flume experiments described here.

The velocity measurement area did not include the scour hole (see Figures 3 and 4b) and it is likely that the secondary flow rapidly decays in the shallow flows over the bartop and downstream of the tributary mixing zone (*cf*. McLelland *et al.*, in press).

One issue not specifically addressed by the flume experiments is the exact mechanism of initial coarse bar deposition in the channel centre. Ashmore (1991, 1993) suggests that initial deposition is through the stalling of a thin (maybe one grain thick) bedload sheet which has been transported down one of the tributaries as a discrete morphological unit. This is consistent with the observations of Carson and Griffiths (1987), who emphasize that most braid–bar material originates from bank erosion and bartail trimming rather than vertical scour and reworking of the bed. Unfortunately, no bedload samples were taken at the initial stages of bar deposition to directly test these ideas (see Ashworth *et al.*, 1992b). However, visual observations suggest that the mid-channel bar did not owe its origin to bedload sheets (Ashmore, 1991) or the local sorting of the bedload (Leopold and Wolman, 1957) but instead to local exceedance of the transport capacity and sediment accumulation in the channel centre by the strongly convergent flow. The overloading of transport capacity occurs early in the flume runs and is caused by the rapid increase in sediment supply through initial junction scour development and entrainment of loose bed and bank material. This situation may also be common in the field when an avulsion creates a new junction scour and the unconsolidated banks rapidly erode as they adjust to the new combined discharge.

Many authors have shown that the confluence–diffluence unit is the fundamental building block of braided rivers (e.g. Carson and Griffiths, 1987; Ashworth *et al.*, 1992a; Bridge, 1993; Goff and Ashmore, 1994). The challenge now is to combine the interpretations and data generated from physical scale models of confluence–diffluence dynamics (e.g. Ashmore, 1991, 1993, this study) with studies of the spatial and temporal patterns of the three-dimensional flow structure (e.g. McLelland *et al.*, in press), bed grain size sorting (e.g. Jackson, 1994), topographic change (e.g. Lane *et al.*, 1994) and two-dimensional bedload transport (e.g. Ashworth *et al.*, 1992a). The quality of data for the latter is probably the poorest and most difficult to obtain, although the response of all factors to a change in flow stage still requires major research.

ACKNOWLEDGEMENTS

This work was undertaken whilst in receipt of a NERC Postdoctoral Fellowship. Professors Chris Paola and Gary Parker kindly allowed access to the flume facilities at St Anthony Falls Hydraulics Laboratory, University of Minnesota. The original idea on velocity switching was put forward by Chris Paola and benefited from discussions with Brian McArdell, Gary Parker and Steve Wiele. I am grateful to the Department of Geology and Geophysics at Minnesota who provided open access to all their facilities during my postdoctoral stay. Philippa Rowling helped with flume data collection and Rob Ferguson with the White River field study. Peter Ashmore, Jim Best, Stuart McLelland and an anonymous reviewer provided many detailed and helpful comments during revision.

REFERENCES

Ashmore, P. E. 1982. 'Laboratory modelling of gravel, braided stream morphology', *Earth Surface Processes and Landforms*, **7**, 201–225.

Ashmore, P. E., 1991. 'How do gravel-bed rivers braid?' *Canadian Journal of Earth Sciences*, **28**, 326–341.

Ashmore, P. E. 1993. 'Anabranch confluence kinetics and sedimentation processes in gravel-braided streams', in Best, J. L. and Bristow, C. S. (Eds), *Braided Rivers*, Geological Society, London, Special Publication, **75**, 129–146.

Ashmore, P. E., Ferguson, R. I., Prestegaard, K. L., Ashworth, P. J. and Paola, C. 1992. 'Secondary flow in anabranch confluences of a braided, gravel-bed stream', *Earth Surface Processes and Landforms*, **17**, 299–311.

Ashworth, P. J. 1988 '*Gravel transport in braided stream systems using a combined field/laboratory approach*', Unpublished Fellowship Report, Natural Environment Research Council, U.K.

Ashworth, P. J. and Ferguson, R. I. 1986. 'Interrelationships of channel processes, changes and sediments in a proglacial river', *Geografiska Annaler*, **68A**, 361–371.

Ashworth, P. J. and Ferguson, R. I. 1989. 'Size selective entrainment of bedload in gravel bed streams, *Water Resources Research*, **25**, 627–634.

Ashworth, P. J., Ferguson, R. I., Ashmore, P. E., Paola, C., Powell, M. D. and Prestegaard, K. L. 1992a. 'Measurements in a braided river chute and lobe: II Sorting of bedload during entrainment, transport and deposition', *Water Resources Research*, **28**, 1887–1896.

Ashworth, P. J., Ferguson, R. I. and Powell, D. M. 1992b. 'Bedload transport and sorting in braided channels', in Billi, P., Hey, R. D., Thorne, C. R. and Tacconi, P. (Eds), *Dynamics of Gravel-Bed Rivers*, John Wiley, Chichester, 497–513.

Ashworth, P. J., Best, J. L., Leddy, J. O. and Geehan, G. W. 1994. 'The physical modelling of braided rivers and deposition of fine-grained sediment', in Kirkby, M. J. (Ed.), *Process Models and Theoretical Geomorphology*, John Wiley, Chichester, 115–139.

Best, J. L. 1986. 'The morphology of river channel confluences', *Progress in Physical Geography*, **10,** 157–174.

Best, J. L. 1988. 'Sediment transport and bed morphology at river channel confluences', *Sedimentology*, **35,** 481–498.

Best, J. L. and Roy, A. G. 1991. 'Mixing layer distortion at the confluence of channels of different depths', *Nature*, **350,** 411–413.

Bluck, B. J. 1979. 'Structure of coarse grained braided stream alluvium', *Transactions of the Royal Society of Edinburgh*, **70,** 181–221.

Boothroyd, J. C. and Ashley, G. M. 1975. 'Process, bar morphology and sedimentary structures on braided outwash fans, northeastern Gulf of Alaska', in Jopling, A. V. and McDonald, B. C. (Eds), *Glaciofluvial and Glaciolacustrine Sedimentation*, Society of Economic Paleontologists and Mineralogists, Special Publication **23,** 193–222.

Bridge, J. S. 1993. 'The interaction between channel geometry, water flow, sediment transport and deposition in braided rivers', in Best, J. L. and Bristow, C. S. (Eds), *Braided Rivers*, Geological Society, London, Special Publication, **75,** 13–71.

Bridge, J. S. and Gabel, S. L. 1992. 'Flow and sediment dynamics in a low sinuosity, braided river: Calamus River, Nebraska Sandhills', *Sedimentology*, **39,** 125–142.

Bristow, C. S. and Best, J. L. 1993. 'Braided rivers: perspectives and problems', in Best, J. L. and Bristow, C. S. (Eds), *Braided Rivers*, Geological Society, London, Special Publication, **75,** 1–11.

Carson, M. A. and Griffiths, G. A. 1987. 'Bedload transport in gravel channels', *Journal of Hydrology (NZ)*, **26,** 1–151.

Cheetham, G. H. 1979. 'Flow competence in relation to channel form and braiding', *Geological Society of America Bulletin*, **90,** 877–886.

Church, M. and Gilbert, R. 1975. 'Proglacial fluvial and lacustrine environments', in Jopling, A. V. and McDonald, B. C. (Eds), *Glaciofluvial and Glaciolacustrine Sedimentation*, Society of Economic Paleontologists and Mineralogists, Special Publication **23,** 22–100.

Church, M. and Jones, D. 1982a. 'Channel bars in gravel-bed rivers', in Hey, R. D., Bathurst, J. C. and Thorne, C. R. (Eds), *Gravel-bed Rivers*, Wiley, Chichester, 291–324.

Church, M. and Jones, D. 1982b. 'Reply to Discussion of "Channel bars in gravel-bed rivers", Jaeggi, M. and Smart, G.', in Hey, R. D., Bathurst, J. C. and Thorne, C. R. (Eds), *Gravel-bed Rivers*, Wiley, Chichester, 334–338.

Colombini, M., Seminara, G. and Tubino, M. 1987. 'Finite-amplitude alternate bars', *Journal of Fluid Mechanics*, **181,** 213–232.

Davoren, A. and Mosley, M. P. 1986. 'Observations of bedload movement, bar development and sediment supply in the braided Ohau River', *Earth Surface Processes and Landforms*, **11,** 643–652.

Dietrich, W. E. 1987. 'Mechanics of flow and sediment transfer in river bends', in Richards, K. S. (Ed.), *River Channels – Environment and Process*, Blackwell, New York, 179–227.

Dietrich, W. E. and Smith, J. D. 1983. 'Influence of the point bar on flow through curved channels', *Water Resources Research*, **19**(5), 1173–1192.

Dietrich, W. E. and Whiting, P. 1989. 'Boundary shear stress and sediment transport in river meanders of sand and gravel', in Ikeda, S. and Parker, G. (Eds), *River Meandering*, American Geophysical Union, Water Resources Monograph **12,** 1–50.

Engelund, F. and Skovgaard, O. 1973. 'On the origin of meandering and braiding in alluvial streams', *Journal of Fluid Mechanics*, **57,** 289–302.

Ferguson, R I. and Ashworth, P. J. 1992. 'Bedload and channel change in braided rivers' in Billi, P., Hey, R. D., Thorne, C. R. and Tacconi, P. (Eds), *Dynamics of Gravel-Bed Rivers*, John Wiley, Chichester, 477–492.

Ferguson, R. I., Prestegaard, K. L. and Ashworth, P. J. 1989. 'Influence of sand on hydraulics and gravel transport in a braided gravel bed river', *Water Resources Research*, **25,** 635–643.

Ferguson, R. I., Ashmore, P. E., Ashworth, P. J., Paola, C. and Prestegaard, K. L. 1992. 'Measurements in a braided river chute and lobe: I. Flow pattern, sediment transport and channel change', *Water Resources Research*, **28,** 1877–1886.

Fredsøe, J. 1978. 'Meandering and braiding of rivers', *Journal of Fluid Mechanics*, **84,** 609–624.

Fujita, Y. 1989. 'Bar and channel formation in braided streams', in Ikeda, S. and Parker, G. (Eds), *River Meandering*, American Geophysical Union, Water Resources Monograph **12,** 417–462.

Goff, J. R. and Ashmore, P. E. 1994. 'Gravel transport and morphological change in braided Sunwapta River, Alberta, Canada', *Earth Surface Processes and Landforms*, **19,** 195–212.

Hassan, M. A. and Church, M. 1992. 'The movement of individual grains on the streambed', in Billi, P., Hey, R. D., Thorne, C. R. and Tacconi, P. (Eds), *Dynamics of Gravel-Bed Rivers*, John Wiley, Chichester, 160–175.

Hein, F. J. and Walker, R. G. 1977. 'Bar evolution and development of stratification in the gravelly, braided, Kicking Horse River, British Columbia', *Canadian Journal of Earth Sciences*, **14**(4), 562–570.

Hoey, T. B. and Sutherland, A. J. 1991. 'Channel morphology and bedload pulses in braided rivers: a laboratory study', *Earth Surface Processes and Landforms*, **16,** 447–462.

Hunt, A. 1994. *Relations between flow velocity, flow direction and bar size in a proglacial Alpine river*, Unpublished B.Sc. dissertation, University of Leeds, U.K.

Jackson, D. J. 1994. *The sedimentology of braided gravel bed rivers*, Unpublished M.Sc. thesis, University of Western Ontario, Canada.

Jaeggi, M. and Smart, G. 1982. 'Discussion of Church, M. and Jones, D. 1982. "Channel bars in gravel-bed rivers" ', in Hey, R. D., Bathurst, J. C. and Thorne, C. R. (Eds), *Gravel-bed Rivers*, Wiley, Chichester, 325.

Krigström, A. 1962. 'Geomorphological studies of sandur plains and their braided rivers in Iceland', *Geografiska Annaler*, **44,** 328–346.

Lane, S. N., Chandler, J. H. and Richards, K. S. 1994. 'Developments in monitoring and modelling small-scale river bed topography', *Earth Surface Processes and Landforms*, **19,** 349–368.

Leddy, J. O., Ashworth, P. J. and Best, J. L. 1993. 'Mechanisms of anabranch avulsion within gravel-bed braided rivers: observations from scaled physical models', in Best, J. L. and Bristow, C. S. (Eds), *Braided Rivers*, Geological Society, London, Special Publication, **75,** 119–127.

Leopold, L. B. and Wolman, M. G. 1957. *River Channel Patterns, Braided, Meandering, and Straight*, United States Geological Survey, Professional Paper **262-B.**

Lisle, T. E., Ikeda, H. and Iseya, F. 1991. 'Formation of stationary alternate bars in a steep channel with mixed-size sediment: a flume experiment', *Earth Surface Processes and Landforms*, **16**, 463–469.

McLelland, S. J., Ashworth, P. J. and Best, J. L., (in press). 'The origin and downstream development of coherent flow structures at channel junctions', in Ashworth, P.J., Best, J.L., Bennett, S. J. and McLelland, S. J. (Eds.), *Coherent Flow Structures in Open Channels: Origins, Scales and Interactions with Sediment Transport and Bed Morphology*, Wiley, Chichester.

Mosley, M. P. 1976. 'An experimental study of channel confluences', *Journal of Geology*, **84**, 535–562.

Mosley, M. P. and Zimpfer, G. L. 1978. 'Hardware models in geography', *Progress in Physial Geography*, **2**, 438–461.

Nelson, J. M. and Smith, J. D. 1989. 'Evolution and stability of erodible channel beds', in Ikeda, S. and Parker, G. (Eds), *River Meandering*, American Geophysical Union, Water Resources Monograph **12**, 321–377.

Paola, C. 1989. 'Topographic sorting', *EOS, Transactions of the American Geophysical Union*, **70**, 332.

Parker, G. 1976. 'On the cause and characteristic scales of meandering and braiding in rivers', *Journal of Fluid Mechanics*, **76**, 457–480.

Parker, G. and Andrews, E. D. 1985. 'Sorting of bed load sediment by flow in meander bends', *Water Resources Research*, **21**, 1361–1373.

Rundle, A. 1985. 'Mechanisms of braiding', *Zeitschrift für Geomorphologie Suppl.-Bd*, **55**, 1–14.

Smith, N. D. 1974. 'Sedimentology and bar formation in the upper Kicking Horse River, a braided meltwater system', *Journal of Geology*, **82**, 205–223.

Smith, N. D. 1978. 'Some comments on terminology for bars in shallow rivers', in Miall, A. D. (Ed.), *Fluvial Sedimentology*, Canadian Society of Petroleum Geologists, Memoir **5**, 85–88.

Southard, J. B., Smith, N. D. and Kuhnle, R. A. 1984. 'Chutes and lobes: newly identified elements in braiding in shallow gravelly streams', in Koster, E. H. and Steel, R. J. (Eds), *Sedimentology of Gravels and Conglomerates*, Canadian Society of Petroleum Geologists, Memoir **10**, 51–59.

Thompson, A. 1986. 'Secondary flows and the pool-riffle unit: a case study of the processes of meander development', *Earth Surface Processes and Landforms*, **11**, 631–641.

Thorne, C. R., Russell, A. P. G. and Alam, M. K. 1993. 'Planform pattern and channel evolution of the Brahmaputra river, Bangladesh', in Best, J. L. and Bristow, C. S. (Eds), *Braided Rivers*, Geological Society, Special Publication, London, **75**, 257–276.

Tubino, M. 1991. 'Growth of alternate bars in unsteady flow', *Water Resources Research*, **27**, 37–52.

Warburton, J. and Davies, T. R. H. 1994. 'Variability of bedload transport and channel morphology in a braided river hydraulic model', *Earth Surface Processes and Landforms*, **19**, 403–421.

Welford, M. R. 1994. 'A field test of Tubino's model of alternate bar formation', *Earth Surface Processes and Landforms*, **19**, 287–297.

Whiting, P. J. and Dietrich, W. E. 1991. 'Convective accelerations and boundary shear stress over a channel bar', *Water Resources Research*, **27**, 783–796.

Williams, P. F. and Rust, B. R. 1969. 'The sedimentology of a braided river', *Journal of Sedimentary Petrology*, **39**, 649–679.

Yalin, M. S. 1971. *Theory of Hydraulic Models*, Macmillan, London.

Yalin, M. S. 1992. *River Mechanics*, Pergamon Press, Oxford.